Medbiotech Journal

MBTJ, 4(2): 87-92, 2020

Research Paper

# Development the Computational Fluid Dynamics in Nanocrystal Technology

**Alisha Saanvi, Rmesh K. Gupta***

Department of Chemistry, Indian Institute for Advanced Materials, India

Received: 11 April 2020 Accepted: 20 May 2020 Published: 01 June 2020

**Abstract**

Chemical vapor transport (CVT)) is known as one of the most efficient methods of synthesizing nanocrystals. In order to investigate the underlying phenomena in CVT processes, especially the growth rate and growth quality in relation to total pressure, temperatures of source and crystal ends, as well as the entangled chemical reactions, CFD modeling is pursued as a powerful and effective tool in lieu of expensive experimental work. CFD modeling has become an important component of the research or a new research methodology and will become increasingly important for simplifying the investigation of phenomena in processes. This paper is presented on how CFD modeling approach can be used as a research methodology in sciences and engineering. Two-dimensional numerical modeling on closed ampoule chemical vapor transport of ZnS–I2 system is conducted. The transport rate (TR) and its transition from diffusion-dominated to convection-dominated regimes in relation to total pressure, average temperature is studied intensively. Modeling results reveal that, the transition of TR from diffusion-dominated to convection-dominated regimes depends on P. Compared to the experimental literature values for all growth regimes, the modeling results agree with the experimental data.

**Keywords:** Research Methodology; Cfd Modeling; Chemical Vapor Transport; Transport Phenomena

***How to cite the article:***

*A, Saanvi, R, K. Gupta, Development the Computational Fluid Dynamics in Nanocrystal Technology, Medbiotech J. 2020; 4(2): 87-92, DOI: 10.22034/MBT.2020.109679.*



## 1.Introduction

Chemical vapor transport (CVT) processes constitute an important technology for manufacturing nanocrystals [1-3] . The production rate or growth of nanocrystals in a CVT ampoule depends on process conditions such as temperature, pressure, reaction kinetic and reactant concentrations. These process conditions can vary throughout the CVT ampoule. The tremendous increase in complexity of nanocrystals products leads to a continuous need for new CVT process and equipment, fulfilling ever increasing performance demands [4-6] . This performance is determined by the interacting influences of hydrodynamics and chemical kinetics in a CVT ampoule, which in turn depend on the process conditions. As a result of this complexity, experimental studies with trial and error methods have always played an important role in CVT process and equipment development. However, the need for a more systematic approach or a new research methodology has been recognized, and has led to the development and application of process models of increasing complexity [7-9] .

Modeling of these systems will provide important aids to the scientific understanding and engineering scale-up of these devices. In particular, CFD modeling should be helpful in interpreting nanocrystal growth rates, transport rates and reaction temperature. Such a CFD

* Corresponding author email: r.gupta.k1983@gmail.com

modeling is the topic of this paper. We present modeling results for the two-dimensional velocity, temperature and transport rate profiles in a two-dimensional CVT ampoule. The geometry is simple, allowing for the easy production of the results, and focused on the CFD modeling as a new research methodology. The chemistry model used is that by ZuO and Wang, which has been extensively documented and tested [10-12] .

## 2. Literature review

Although many experimental studies on transport phenomena in closed ampoules have appeared in the literature, most of them are for physical vapor transport (PVT) [5-6], there are few modeling studies on CVT [3,4]. Although the modeling results on PVT provide a good reference frame, they cannot simply be applied, without differentiation, to CVT processes for the following reasons. (1) Unlike PVT, carrier gas in CVT is no longer inert but will react with source and crystal surfaces, thus both mass flux and mass concentration on the two surfaces are much different from that derived in PVT. (2) In PVT with the carrier gas present, system pressure usually varies slightly around 0.05 atm and temperature difference between the two ends is usually less than 10K, which often results in either diffusion-dominated or convection dominated transport modes. While in CVT, pressure is usually in the order of 1 atm, temperature difference varies from as small as 3K to as large as 500K, but mostly around 10–100K. For these reasons flow patterns and transport modes in CVT are different from that in PVT. (3) Because of the small temperature and pressure variations in PVT, the compressibility effect is usually neglected and thermo physical parameters can be assumed constant. While in CVT, due to large differences in temperature and pressure that usually occur, the compressibility effect and variations of thermo physical parameters with temperature and pressure can no longer be ignored and have to be considered. Comparisons between PVT and CVT in relation to transport phenomena are listed in table 1.

For modeling of an enclosure filled with vapor with differentially heated end walls (Figure 1), there are mainly four approaches to build the velocity boundary condition at the source and crystal surfaces. The first is to totally ignore the effect of interfacial mass transport that corresponds to the case of pure thermal convection induced by the differentially heated end walls (the effect of concentration gradient being neglected). The second is to impose a fixed velocity at the interface [13-15] . It involves an arbitrarily chosen proportional factor and, in general, is not easily used. The third is to relate the interfacial velocity to the concentration gradient by considering species conservation at the interface with inert carrier gas condition, which was derived by Rosenberger et al. [13, 14] and has been widely used for PVT processes [1, 16-19] . The fourth is a non-equilibrium, surface kinetics-related boundary condition, which was derived by Zappoli et al. [1, 18, 19] and was used in a two-dimensional rectangular model of the GeI2/GeI4 CVT system.

**Table 1.** Comparisons between PVT and CVT in relation to transport phenomena

| Parameters | Physical vapor transport (PVT) | Chemical vapor transport (CVT) |
|---|---|---|
| **Growth mechanism Carrier gas** | Monatomic, associative Inert | Reversible chemical reactions Reacting |
| **Growth temperature (T)** | Sublimation point (typical 1000 K) | Typical 100K less than sublimation point |
| **Temperature difference** | 1–10 K | 3–500K, 1–3atm |
| **Total system pressure** | High vacuum or inert gas | Varying |
| **Thermo physical parameters** | Constant | Significant |
| **Compressibility effect Aspect ratio (L/d)** | Insignificant, Typical 5 | Typical 10 |

However, because of the complicated surface kinetics involved, the boundary condition of this model is hard to apply to the general CVT process at chemical equilibrium conditions. It is the purpose of this paper to explore the underlying phenomena in the kinetic process of closed ampoule CVT, especially the relationship between the bulk diffusion/advection. In doing so, we try to develop a general expression for the mass transport rate and a widely accepted velocity boundary condition at the vapor/solid interface.

In the study, we concentrate on the kinetic process of the ZnS–I2 system, because this system has been most widely studied and has the most data available. Specifically, under the condition of equilibrium chemical reactions, partial pressures of various species near the source and crystal surfaces will be determined. By considering species conservation at the solid/vapor interface

in relation to stoichiometric chemical reactions, the expressions of transport rate and mass average velocity in the vapor/solid interface will be established and will later be used in solving coupled conservation equations for the general two-dimensional CVT process. Furthermore, we present experimental validations of the model with published data.

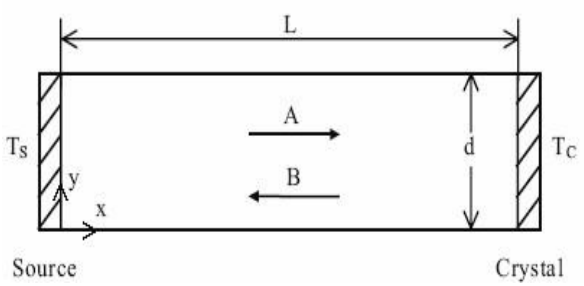


**Figure 1.** Schematic and coordinates of closed ampoule

## 3. Chemical reactions and partial pressures

Due to chemical reactions occurring at the source and crystal ends in the CVT ampoule, species in the vapor mixture are either created or destroyed in the vapor/solid interface (assuming the gas phase reaction to be neglected). Thus, partial pressures in the ampoule are affected strongly by heterogeneous chemical reactions. In order to construct a physical model for mass transport, we need to consider the specific chemical reactions in equilibrium at the source and crystal surfaces so as to determine the species partial pressures and consequently the velocity and mass transport rate expressions for the CVT system. In CVT process, diatomic iodine $I_2$ is widely used as a carrier gas (transport agent). We consider the $ZnS$–$I_2$ system at temperatures between 1000 and 1100 K, which covers the actual crystal growth temperature range from previous experimental practices. In this temperature range, the following species exist in significant amount in the vapor phase: $I_2$, $I$, $ZnI_2$ and $S_2$, other gas species such as $ZnI$, $Zn$ and $S$ are tiny and can be neglected. Thus, we consider the following reactions occurring simultaneously in the system:

ZnS + I2 = ZnI2 + 1/2S2 (R1)

ZnS + 2I = ZnI2 + 1/2S2 (R2)

I2 = 2 I (R3)

## 4. CFD model

### *4.1. Ampoule model*

We adopt a horizontal rectangular enclosure with two vertical end walls (source and crystal ends) fixed at different temperatures as our physical model (Figure 1). The width of the enclosure is assumed much larger than the height. In this way, we can ignore the dimension of width and use a two-dimensional rectangular model to simulate the vertical mid-plane of a real three-dimensional cylindrical ampoule. Consider the enclosure filled with a vapor mixture consisting of mainly four species: $I_2$, $I$, $ZnI_2$ and $S_2$.

### *4.2. Transport model*

To find the transport rate of $ZnI_2$ particles and the influencing parameters, we need to solve the coupled conservation equations of mass, momentum, species and energy in steady state. Since there exists a rather high temperature (1000–1100 K) and temperature difference (100 K) in the common CVT system, density change is significant and Boussinesq approximation is no longer valid. In order to minimize the modeling errors, general conservation equations including the compressibility effect and the varying thermo physical parameters with temperature and pressure are adopted. According to Patankar [10], the four partial differential equations from the conservation laws can be represented by the generic equation:

$$\Delta.(\rho u \varphi) = \Delta.(\Gamma \Delta \varphi) + S \qquad (4)$$

where $\Delta = \partial / \partial x + \partial / \partial y$, $\varphi$ represents the corresponding variable in each conservation equation, and all other terms are assumed constant during each numerical interpolation step. The terms in equation *(4)* for different conservation equations are listed in table 2. Since $I_2$ particles are no longer inert, but penetrate into or out of the source or crystal surface and react with the surface, both velocity and mass component boundary conditions are different from that in PVT. The boundary conditions for velocity, temperature and mass components can be expressed as follows (w denoting $w_A$ for convenience).

Source end,

u (0, y) = f (∂w / ∂x), v (0 , y ) = 0, T ( 0 , y ) = Ts, w (0 , y ) = f ( Mi , P ) (5)

Crystal end,

u (L, y) = f (∂w / ∂x), v (L, y ) = 0, T ( L , y ) = Tc, w (L, y ) = f ( Mi , P ) (6)

Walls,

u (0 , y ) = u (L , y ) = 0, v ( 0 , y ) = v ( L , y ) = 0, T ( 0 , y ) = T ( L , y ) = Ts – (Ts – Tc )x/L w ( 0 , y ) = (7)
w ( L , y ) = ws – (ws – wc )x/L

**Table 2.** Variables and constants corresponding to Eq. (4) in different conservation equations

| | $\varphi$ | $\Gamma$ | $S$ |
|---|---|---|---|
| **Mass conservation** | *1* | 0 | 0 |
| **x-momentum conservation** | u | μ | $\partial \rho/\partial x$ |
| **y-momentum conservation** | *v* | μ | $\partial \rho/\partial y - \rho g y$ |
| **Energy conservation** | *T* | k/c | 0 |
| **Mass component conservation** | *w* | $\rho D$ | $\partial w/\partial x$ |

Conservation equations in the form of equation *(4)* with boundary conditions equations (5) – (7) are solved with a finite volume computer code SIMPLE [10]. The grid mesh is 50 * 100. The program is run on a PVI PC. In each calculation, depending upon the total pressure parameter, it takes about 1500–2500 iterations to reach convergence.

### *4.3. Gas properties*

The above model equations comprise thermo-chemical (specific heat, heat of formation and entropy) and transport (viscosity, thermal conductivity and diffusivities) properties of the gas mixture in the ampoule. Thermochemical properties of gases can be found in e.g. [20-22] . Here, we have used the thermo-chemical properties as a function of temperature. The transport equations and the calculation of thermo-chemical and transport properties apply generally to multicomponent gas mixtures at moderate temperature and pressure.

## 5. Modeling results and discussions

### *5.1. Transport rate as function of total system pressure*

The variation of transport rate (TR) with system pressure (P) is depicted in Figure 2. This figure also gives the comparison between the modeling results and the experimental ones from the literature. The TR are calculated and averaged over the whole crystal surface (over y-direction). The continuous curves are drawn form discrete calculations of TR at each individual pressure at selected ampoule geometry and temperature. The calculated transport rates in Figure 2 are compared with the experimental ones from Dangel and Wuensch [6] for the same growth conditions. Figure 2 shows that the predicted values agree qualitatively with the experimental ones for entire pressure range. Although the predicted TR values are approximate, give good predictions for the transition points from the diffusion-dominated to convection- dominated regimes.

### *5.2. Flow pattern, flow transition and flux transition*

From numerical modeling results, we find that the transition of transport rate is different from the transition of flow pattern. To distinguish the two different transitions, we call the former the flux transition and the latter the flow transition.

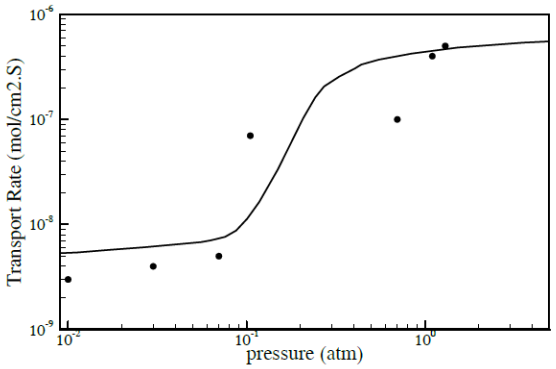


**Figure 2.** Transport rate as a function of total pressure, Discrete points are the experimental data, Ref. [4].

Figures 3-5 show the changes of flow patterns from pure diffusion/advection (*P = 0.01* atm) to flow transition (*P= 0.03* atm) and to full circulatory convection *(P= 0.1* atm) for *d = 1.5* cm, *L = 14* cm, *Ts = 1063K* and *Tc =1013K* condition. Comparing to Figure 2, we find that at the same growth condition, the flow transition occurs at much lower pressure (*P= 0.03* atm) than the flux transition (*P= 0.4* atm), i.e., the flow may be in circulatory convection while the transport may still be dominated by the diffusion/advection mode. By determining the onset pressure for flow transition at different growth conditions (Figure 2), it is estimated that the pressure for flow transition is about *1/13* of that for flux transition under the same temperature and geometric conditions. To extend this result, more numerical calculations for higher temperature differences are needed.

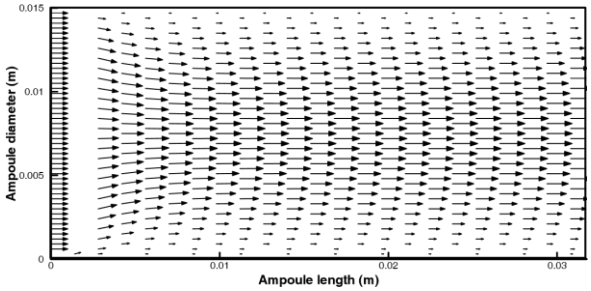


**Figure 3.** Flow patterns for pure diffusion.

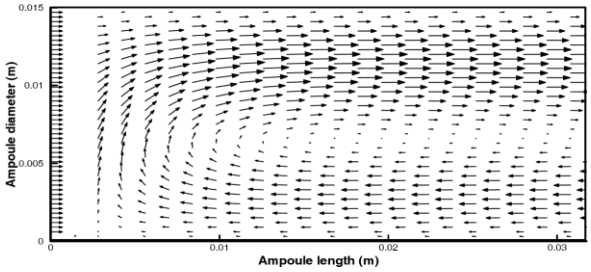


**Figure 4.** Flow patterns for flow transition from pure diffusion/advection to full circulatory convection (P=0.03 atm, others are the same as in Figure 3).

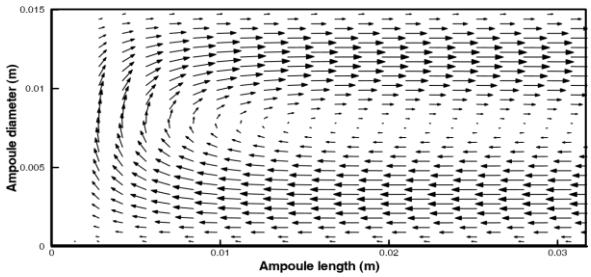


**Figure 5.** Flow patterns for full circulatory convection near the two ends.
(P=0.1 atm, others are the same as in Figure 3).

## 6. Conclusion

Apart from costly and time-consuming experimental research methods, in this paper, CFD modeling as a new research methodology in CVT processes is presented. Two dimensional simulations have been presented of the multicomponent transport phenomena and the multispecies, multi-reaction gas phase chemistry in a CVT ampoule. A detailed description has been given of the problem definition and the model equations and parameters. Compared to the experimental literature values for all growth regimes, the modeling results agree with experimental ones qualitatively in TR values and accurately in the transition of TRs.

By using CFD modeling to investigate how several parameters influence the CVT ampoule, a greater understanding of this process has been achieved. The new knowledge has been used to optimize the process design to give optimum conditions. Thus, this paper illustrates the potentials of CFD modeling to predict and optimize CVT process characteristics.

## References

1. Santharaman P, Venkatesh KA, Vairamani K, Benjamin AR, Sethy NK, Bhargava K, et al. 2017. ARM-microcontroller based portable nitrite electrochemical analyzer using cytochrome c reductase biofunctionalized onto screen printed carbon electrode. *Biosensors and Bioelectronics* 90: 410-417.

2. Hwang J-Y, Shin US, Jang W-C, Hyun JK, Wall IB, Kim H-W. 2013. Biofunctionalized carbon nanotubes in neural regeneration: a mini-review. *Nanoscale* 5(2): 487-497.

3. Basak G, Hazra C, Sen R. 2020. Biofunctionalized nanomaterials for in situ clean-up of hydrocarbon contamination: A quantum jump in global bioremediation research. *Journal of Environmental Management* 256: 109913.

4. Torres-Martínez CL, Nguyen L, Kho R, Bae W, Bozhilov K, Klimov V, et al. 1999. Biomolecularly capped uniformly sized nanocrystalline materials: glutathione-capped ZnS nanocrystals. *Nanotechnology* 10(3): 340-354.

5. Kar S, Biswas S, Chaudhuri S. 2005. Catalytic growth and photoluminescence properties of ZnS nanowires. *Nanotechnology* 16(6): 737-740.

6. Kheirabadi MA, Jafari MH, Alizadeh F, Basiri Z, Oveisi K. 2019. Comparison and Satisfaction of Injured Management System for Students Athlete in the Sport Federations. *Journal of Computational and Theoretical Nanoscience* 16(1): 284-288.

7. Yaghoubi Nezhad A, Soltantabar Shahabedini A, Ali H. 2020. Determination of small amounts of fluoxetine in a biological sample through solid phase extraction method by carbon nanotubes. *Eurasian Chemical Communications*. en.

8. Esmaeilimotlagh M, Basiri Z, Kheirabadi MA, Oveisi K. 2019. The Effect of Information and Communication Technology on the Professional Development of Teachers. *Journal of Computational and Theoretical Nanoscience* 16(1): 312-318.

9. Jafari MH, Kashisaz S, Manna M. 2019. Effects of Nanoparticles on the Durability and Mechanical Properties of Concrete. *Journal of Computational and Theoretical Nanoscience* 16(1): 275-283.

10. Shamsin Beyranvand H, Mirzaei Ghaleh Ghobadi M, Sarlak H. 2020. Experimental Study of Carbon Dioxide Absorption in Diethyl Ethanolamine (DEEA) in the Presence of Titanium Dioxide (TiO2). *Progress in Chemical and Biochemical Research* 3(1): 55-63. en.

11. Joo J, Na HB, Yu T, Yu JH, Kim YW, Wu F, et al. 2003. Generalized and Facile Synthesis of Semiconducting Metal Sulfide Nanocrystals. *Journal of the American Chemical Society* 125(36): 11100-11105.

12. Hu J, Bando Y, Zhan J, Golberg D. 2005. Growth of Wurtzite ZnS Micrometer-Sized Diskettes and Nanoribbon Arrays with Improved Luminescence. *Advanced Functional Materials* 15(5): 757-762.

13. Li LS, Pradhan N, Wang Y, Peng X. 2004. High Quality ZnSe and ZnS Nanocrystals Formed by Activating Zinc Carboxylate Precursors. *Nano Letters* 4(11): 2261-2264.

14. Jiang Y, Meng X-M, Liu J, Xie Z-Y, Lee C-S, Lee S-T. 2003. Hydrogen-Assisted Thermal Evaporation Synthesis of ZnS Nanoribbons on a Large Scale. *Advanced Materials* 15(4): 323-327.

15. Safoora Eissazadeh MHJ, Sara Kashisaz, Mohsen Manna. 2019. Investigation into the Behavior of Square Concrete-Reinforced Columns Under Axial Loading, Retrofitted by Fiber-Reinforced Polymer and Steel Jacket. *Journal of Computational and Theoretical Nanoscience* 16(01): 295-307.
16. Hao Y, Meng G, Wang ZL, Ye C, Zhang L. 2006. Periodically Twinned Nanowires and Polytypic Nanobelts of ZnS: The Role of Mass Diffusion in Vapor−Liquid−Solid Growth. *Nano Letters* 6(8): 1650-1655.
17. Ma J, Huang X, Cheng H, Zhao Z, Qi L. 1996. Preparation of nanosized ZnS particles in water/oil emulsions by microwave heating. *Journal of Materials Science Letters* 15(14): 1247-1248.
18. Zhang D, Qi L, Cheng H, Ma J. 2002. Preparation of ZnS Nanorods by a Liquid Crystal Template. *Journal of Colloid and Interface Science* 246(2): 413-416.
19. Jun Y-w, Choi J-s, Cheon J. 2006. Shape Control of Semiconductor and Metal Oxide Nanocrystals through Nonhydrolytic Colloidal Routes. *Angewandte Chemie International Edition* 45(21): 3414-3439.
20. Calandra P, Goffredi M, Liveri VT. 1999. Study of the growth of ZnS nanoparticles in water/AOT/n-heptane microemulsions by UV-absorption spectroscopy. *Colloids and Surfaces A: Physicochemical and Engineering Aspects* 160(1): 9-13.
21. Ferreira GMD, Ferreira GMD, Almeida GWR, Soares NFF, Pires ACS, Silva LHM. 2019. Thermodynamics of multi-walled carbon nanotube biofunctionalization using nisin: The effect of peptide structure. *Colloids and Surfaces A: Physicochemical and Engineering Aspects* 578: 123611.
22. Bredol M, Merikhi J. 1998. ZnS precipitation: morphology control. *Journal of Materials Science* 33(2): 471-476.